Study of universality at integer quantum Hall transitions

2000 J. Phys.: Condens. Matter 12 5343

(http://iopscience.iop.org/0953-8984/12/25/301)

J. Phys.: Condens. Matter **12** (2000) 5343–5360. Printed in the UK PII: S0953-8984(00)12194-0

Study of universality at integer quantum Hall transitions

Kun Yang†, D Shahar‡, R N Bhatt, D C Tsui and M Shayegan

Department of Electrical Engineering, Princeton University, Princeton, NJ 08544, USA

E-mail: kunyang@magnet.fsu.edu

Received 1 March 2000

Abstract. We report in this paper results of experimental and theoretical studies of transitions between different integer quantum Hall phases in two-dimensional electron systems, as well as the transition to the insulating phase at high magnetic fields. We focus mainly on the resistivity at the transitions. We first present results of a numerical calculation for a non-interacting electron model, which shows that the Thouless conductance is universal at integer quantum Hall transitions, just like the conductivity tensor. We then present experimental results for the measured longitudinal resistivity at the quantum Hall–insulator transition, which are found to be clustered around the universal value suggested theoretically for the non-interacting model, within a range of 15%. Finally, we investigate departure from universality due to finite temperature and finite system size near the transition point.

1. Introduction

Continuous (or second-order) quantum phase transitions in many-electron systems are of general interest to condensed matter physicists [1]. Recently a class of such quantum phase transitions, namely the transitions between different quantum Hall plateaus, and the transition between a quantum Hall phase and an insulating phase at high magnetic field (B), have been under extensive experimental [2–15] and theoretical [16–40] study. These transitions are realized in a variety of two-dimensional electron systems (2DES) formed at the interface between two semiconductors, or in semiconductor quantum well structures.

In the renormalization group (RG) language, continuous phase transitions are controlled by RG fixed points, and many properties of the transition depend only on which fixed point the transition is controlled by, or which universality class it belongs to, and are independent of microscopic details of the system. The best known examples of such universal properties are of course the critical exponents. In principle, other quantities that are dimensionless can also be universal at the critical point. Of particular interest in the study of quantum Hall transitions is the conductivity tensor at the critical point, which in two dimensions (2D) can be expressed as dimensionless numbers times the fundamental unit of conductance, e^2/h. It has been suggested that these numbers should be universal, both at superfluid–insulator transitions [41], and quantum Hall transitions [19]. In the latter case, which is the focus of the present paper, this suggestion has received some support from both experimental [9, 11] studies at the quantum Hall–insulator transition at high magnetic field, and numerical work in

† Present address: National High Magnetic Field Laboratory and Department of Physics, Florida State University, Tallahassee, FL 32306, USA.

‡ Present address: Department of Condensed Matter Physics, Weizmann Institute, Rehovot 76100, Israel.

0953-8984/00/255343+18$30.00

the lowest Landau level [20] as well as the network model [28, 29]. However, experimentally it was found [11] that there exists some scatter in the data around the predicted universal value. Also experimentally there is evidence [42] that critical scaling may not hold if all data in a broad temperature range are used. The issue is therefore not yet settled.

In this paper, we further address the issue of universality of the conductance tensor at the quantum Hall transitions, which was considered in previous work by our group [11, 20]. We present new results of a numerical study of the integer quantum Hall transitions for a non-interacting electron model on a lattice. Our results show that another dimensionless quantity, the Thouless conductance, a quantity that is closely related to the longitudinal conductance of the system, is universal at integer quantum Hall transitions. We then present results of further experimental studies of the resistivity tensor at the integer quantum Hall transitions. In agreement with previous experimental work, we find, at the transition between the $\nu = 1$ quantum Hall state and the insulator at high magnetic field, that the longitudinal resistivity, ρ_{xxc}, is indeed clustered around the theoretically suggested universal value, h/e^2, but the data show a scatter of order 15%. Possible sources of this scattering will be discussed. No such scattering is found in the critical Hall resistivity, ρ_{xyc}.

The above results pertain to the infinite system in the limit of $T = 0$. We then consider the effect of non-zero temperature (for the experimental data) and the effect of finite size (numerical calculation). We present data on the T-dependence of ρ_{xx} at the critical point, and study how the asymptotic zero-temperature value is reached. In a *non-interacting* system, the effect of a finite T is to set a finite dephasing length, which effectively divides an otherwise infinite system into incoherent finite pieces, and introduces finite-size effects to the critical behaviour. We have therefore also studied the size dependence of the Thouless conductance near the critical points, in our numerical calculations, in an effort to see the relation with experimental observations of finite-temperature effects in the true interacting electron gas in two dimensions.

The rest of the paper is organized as described below. In section 2 we present results of our numerical study on a non-interacting electron model on a lattice, and demonstrate that at the critical points, the properly defined Thouless conductance is a universal number that is independent of the strength and type of random potential, amount of mixing between different Landau levels (subbands), whether there is particle–hole symmetry, etc. We also study the system size dependence of the Thouless conductance at the critical points, and demonstrate that the universal asymptotic value is reached at surprisingly small system sizes in the lowest Landau subband. In section 3 we present our experimental results on studies of the resistivity tensor, both at the high-field QH–insulator *and* QH–QH critical points. We study both the asymptotic low-temperature behaviour, and how the asymptotic values are approached, by studying the temperature dependence at higher temperature. In section 4 we discuss the relation between our experimental and numerical results, as well as their connection to other theoretical and experimental work.

2. Numerical study of Thouless conductance

In this section we present results of numerical studies of the Thouless conductance at the critical point, using a non-interacting electron model on a square lattice, described by the following Hamiltonian:

$$H = \sum_{m,n} \{-(c^\dagger_{m+1,n} c_{m,n} + c^\dagger_{m,n+1} \mathrm{e}^{\mathrm{i}\,2\pi\alpha m} c_{m,n} + \mathrm{H.c.}) + \epsilon_{m,n} c^\dagger_{m,n} c_{m,n}\} \tag{1}$$

where the integers m and n are the x- and y-coordinates of the lattice site in terms of the lattice constant, $c_{m,n}$ is the fermion operator on that site, H.c. stands for Hermitian conjugate, α is the

amount of magnetic flux per plaquette in units of the flux quantum hc/e, and ϵ is the random on-site potential. We will present data mostly for an uncorrelated random potential (i.e., no correlation between ϵs on different lattice sites), with ϵ ranging uniformly from $-W$ to W. A random potential with some short-range correlation will also be studied. The Landau gauge $\boldsymbol{A} = (0, Bx, 0)$ is used in equation (1). In this work we study finite-size systems of square geometry, with linear size L, for L ranging from 18 to 50. We impose a periodic boundary condition (PB) along the $\hat{x}$-direction: $\Psi(k + L\hat{x}) = \Psi(k)$ and a periodic or antiperiodic boundary condition (APB) along the $\hat{y}$-direction: $\Psi(k + L\hat{y}) = \pm\Psi(k)$. We diagonalize the Hamiltonian (1) numerically to obtain the single-electron spectrum for both the periodic boundary condition (E_p^n) and the antiperiodic boundary condition (E_{ap}^n) along the $\hat{y}$-direction, while keeping the boundary condition along $\hat{x}$ periodic. Here n is the index for a specific eigenstate.

The Thouless conductance [43] at Fermi energy E is defined as

$$g_T(E) = \frac{\langle \delta E \rangle}{\Delta E} \tag{2}$$

where $\Delta E = 1/[L^2 D(E)]$ is the average level spacing at E, determined by the disorder-averaged density of states (DOS) per site $D(E)$, and $\langle \delta E \rangle$ is the average of the absolute values of the difference between E_p^n and E_{ap}^n, also at energy E†.

In figure 1 we show the Thouless conductance (g_T) for systems with $\alpha = 1/3$, $W = 2.5$ (uncorrelated potential), and L ranging from 18 to 48. We find, except for four special energies, that g_T *decreases* as L increases; while for $E = \pm E_c^1 \approx \pm 2.0$ and $E = \pm E_c^2 \approx \pm 1.1$, g_T

† There are different ways to define the Thouless conductance. For example, reference [25] uses the geometric mean instead of the ordinary average of the energy difference to determine $\langle \delta E \rangle$. What we mean by the universality of Thouless conductance is that for a fixed definition, like the one used in this paper, the Thouless conductance at the critical point is independent of the details of the model.

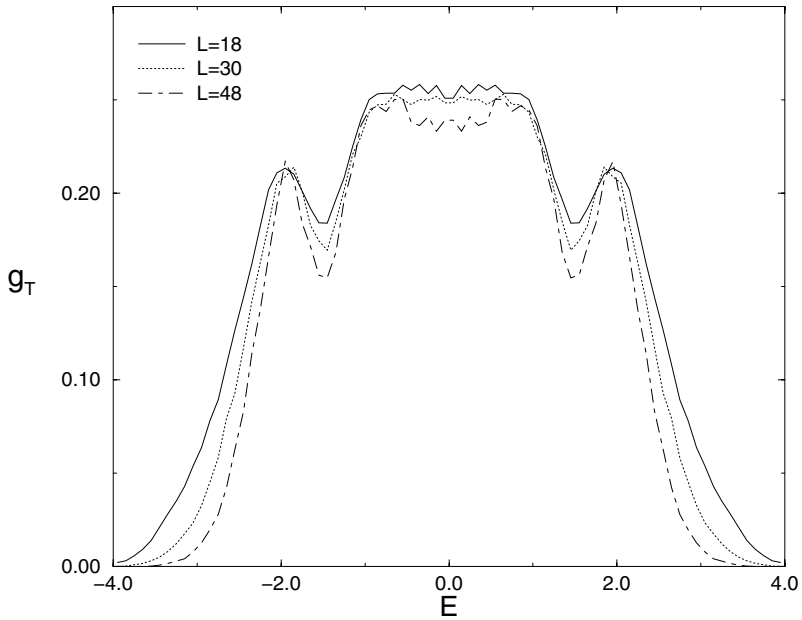

Figure 1. Thouless conductance g_T as a function of energy for $\alpha = 1/3$, $W = 2.5$, at different system sizes.

peaks, and appears to be essentially *independent* of L†. The physics of such behaviour may be understood in the following way [31–34, 36]. In the absence of a random potential we have three Landau subbands, and the Hall conductance (in units of e^2/h) for each subband is 1 for the two side bands and -2 for the central band. As the random potential is turned on, most states get localized, but there will be one critical energy in each side band ($\pm E_c^1$) and two critical energies ($\pm E_c^2$) in the central band, at which states are delocalized. The Hall conductance carried by the extended states is 1 for $\pm E_c^1$, and -1 for $\pm E_c^2$. For energies away from these critical energies, states are localized; therefore g_T decreases as system size L increases, and goes to zero in the thermodynamic limit; at these critical energies, states are delocalized, and g_T approaches a finite number in the thermodynamic limit; for large enough system size L, g_T is essentially independent of L. It is clear from the plot that g_T has essentially reached its asymptotic value for $L \geqslant 18$; the size dependence of g_T at smaller sizes will be discussed later. E_c^1 and E_c^2 move together as W increases, and at $W = W_c \approx 2.9$ they merge together and annihilate each other, and all states become localized [33].

In the following we will focus on the value of g_T at the critical energies. In figure 2(a) we show the size-independent peak value of g_T at $E = -E_c^1$, for different randomness strengths W, and $L = 30$ (which we believe to be in the asymptotic regime already). The value of g_T is the same at $E = E_c^1$, due to the particle–hole symmetry of the model. We find $g_T \approx 0.21 \pm 0.02$, *independent* of the value of W. In figure 2(b) we present the peak value of g_T in the lowest Landau subband for $\alpha = 1/5$ and $\alpha = 1/7$, at different Ws, and system sizes $L = 25$ and $L = 21$ respectively. We have checked that for these sizes the peak value of g_T of the lowest Landau subband is already at its asymptotic value. Again we get the same value, within error bars, even though we have different field strengths and different numbers of Landau subbands.

So far we have only studied uncorrelated random potentials on the lattice, which maps onto a Gaussian white-noise potential in the continuum limit. In the following we study random potentials with short-range correlations. We use the following way to generate short-range correlation: we generate an uncorrelated random number w_i, uniformly distributed from $-W$ to W, for each lattice site i. Instead of using w_i as the random on-site potential ϵ_i as before, we take

$$\epsilon_i = w_i + a \sum_{\delta} w_{i+\delta} \tag{3}$$

where the summation is over the four neighbouring sites of i. This way, the potential of one site is correlated with its nearest and next-nearest neighbours, and the amount of correlation is determined by a. In figure 3 we show the size-independent peak value of g_T (again based on data with $L = 30$) at E_c^1, for $\alpha = 1/3$, $W = 1.5$, at different as. We find that within error bars it is independent of a, and takes the same value as the uncorrelated potential ($a = 0$).

Our data clearly indicate that $g_T \approx 0.21 \pm 0.02$ is a universal number at the critical energy of the lowest Landau subband of the square lattice, independent of the strength of the randomness and magnetic field, as well as the type of random potential (correlated or uncorrelated). Within error bars, the same universal number is also found in the lowest Landau level of the *continuum system* in reference [37], as well as by others [38], where the same definition of the Thouless conductance was used. We point out however that in our calculation, no projection to individual subbands is made, and mixing between different Landau subbands (or levels) (which is often important in real systems) is taken into account. We thus conclude that just like the conductivity tensor, the Thouless conductance is a universal number at integer quantum Hall transition in non-interacting electron models (either on a lattice or in the continuum).

† The independence of g_T of L is quite clear for $E = \pm E_c^1$, while at $\pm E_c^2$ there appears to be some very weak L-dependence. On the basis of previous studies (see below), we know that there should be two critical energies at $\pm E_c^2$. The weak size dependence of g_T on L will be discussed later.

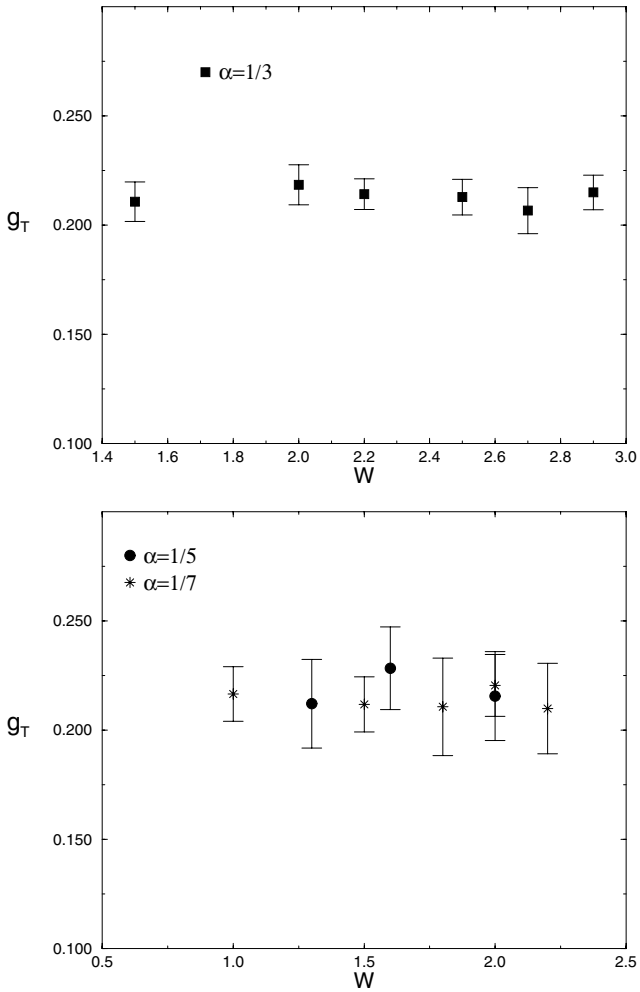

Figure 2. The peak value of the Thouless conductance g_T in the lowest Landau subband, for different magnetic field (α) and randomness (W) strengths, with an uncorrelated random potential.

In principle, the truly universal value of g_T at the critical energies is reached in the thermodynamic limit $L \to \infty$ only; there is always finite-size correction of g_T at finite L, and the correction should decrease as L increases. As discussed in section 1, in a non-interacting system a finite system size is equivalent to finite temperature in an infinite system. Since real experiments are always done at finite temperatures, such finite-size effects are observable. Motivated by this we have also studied the size dependence of g_T at the critical energies. In figure 4 we plot the dependence of g_T at $E = -E_c^1$ for $\alpha = 1/3$ and $W = 2.5$. We find, quite remarkably, that for L as small as 9, g_T has essentially saturated at the asymptotic value, indicating that the finite-size corrections of g_T disappear extremely fast as L increases. The deviation of g_T at $L = 6$ from the universal value is clearly due to finite-size corrections; associated with that, we have also found strong dependence of the peak value of g_T at $L = 6$ on the randomness strength W, as shown in figure 5. We find the bigger W is, the closer to the universal value g_T becomes. This is reasonable because the stronger randomness is more

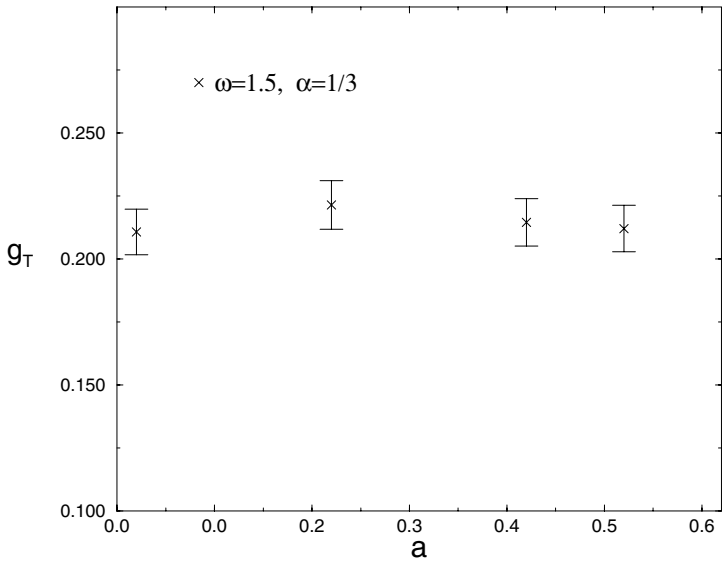

Figure 3. The peak value of the Thouless conductance g_T in the lowest Landau subband for a short-range correlated potential. a is the strength of the short-range correlation.

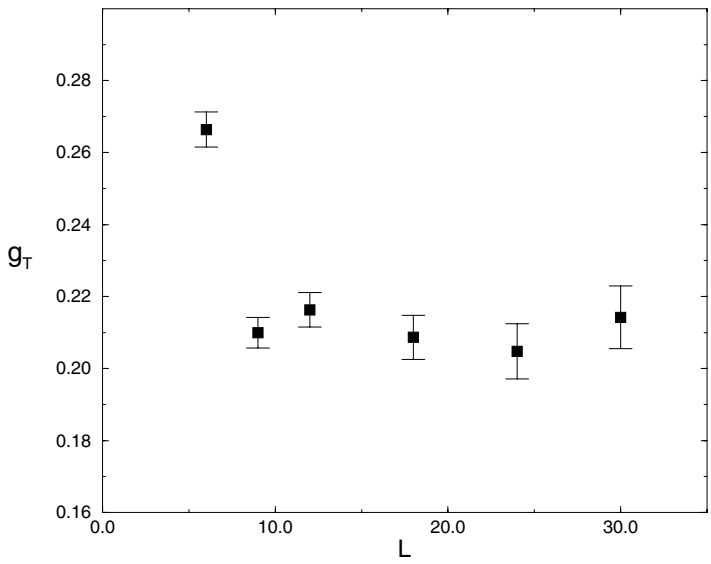

Figure 4. The L-dependence of g_T at the critical energy of the lowest Landau subband for $\alpha = 1/3$.

effective in localizing states away from critical energies, and therefore suppresses finite-size effects. No such dependence on W, however, is found for larger L where g_T has saturated at the universal value.

In the RG language, the finite-size correction to universal properties at the critical point is due to the existence of irrelevant operators, whose strength scales to zero in the thermodynamic limit under the RG at the critical point, while they remain finite in finite-size systems. It has

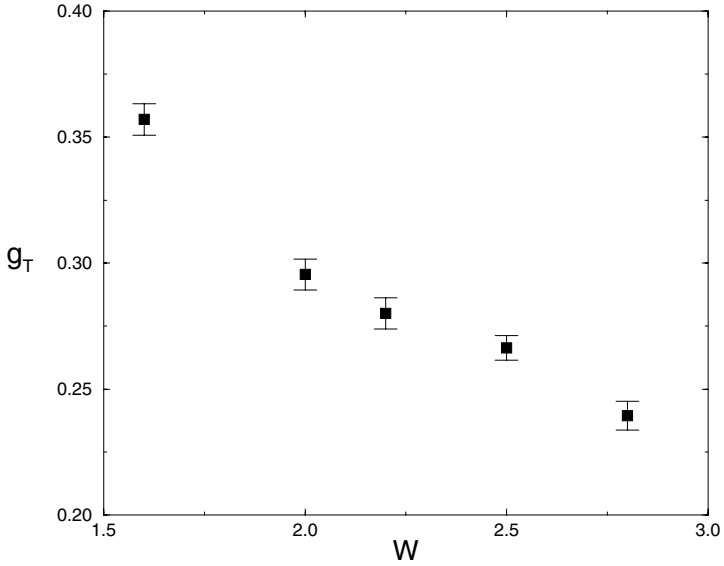

Figure 5. The peak value of g_T (at $E = -E_c^1$) in the lowest Landau subband for $\alpha = 1/3$ and $L = 6$ versus randomness strength W.

been known [44] for some time now, on the basis of numerical studies, that the length scale required for such irrelevant operators to scale away is quite small in the lowest Landau level, while in higher Landau levels it becomes very large. The origin of this difference is not yet fully understood. Our result in the lowest Landau subband is clearly consistent with this finding. Also consistent with this, we do see some weak size dependence of the peak value of g_T in higher subbands (see figure 1), suggesting the existence of finite-size correction in the size range of our numerical study. We have also found strong dependence of the peak value of g_T in higher subbands on W for a given size as shown in figure 6. The dependence is very similar to that of the peak value of g_T in the lowest subband with $L = 6$, where we know that finite-size corrections are present. Based on these we conclude that finite-size corrections are quite important in higher Landau subbands within the size range of the present study, and conjecture that in the thermodynamic limit, the peak value of g_T may saturate at the same universal value as in the lowest subband, provided that the critical energy carries Hall conductance ± 1. We will discuss the possible experimental consequences of these finite-size effects in section 4.

3. Experiments

In this section we describe our experimental results. While our main finding has already been published before [11], we present here a more detailed account of our study of the QH-to-insulator phase transition at low T. Since the main motivation of our work was to test the theoretically predicted *universal* features, we have set out to study a broad range of samples that represents much of the available variety of 2DES samples at the time of carrying out this work. In figure 7 we illustrate this large diversity of samples studied by plotting the mobility (μ) versus density (n) for some of our samples. The range of the axes in this figure is chosen to represent virtually the entire range of 2DES that is reported in the literature ($\mu = 10^3$–10^7 cm^2 V^{-1} s^{-1} and $n = 10^9$–10^{12} cm^{-2}). As can be seen, our samples cover a significant area in this log–log graph. To increase the generality of our results we obtained our samples

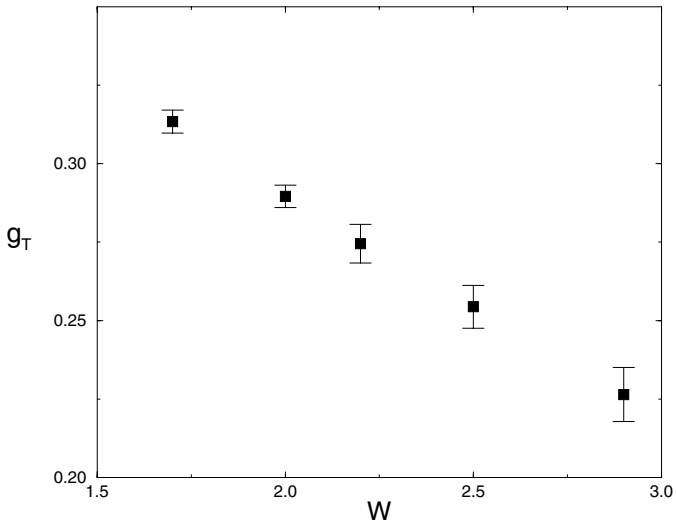

Figure 6. The peak value of g_T (at $E = -E_c^2$) in the central Landau subband for $\alpha = 1/3$ and $L = 30$ versus randomness strength W (E_c^2 depends on W).

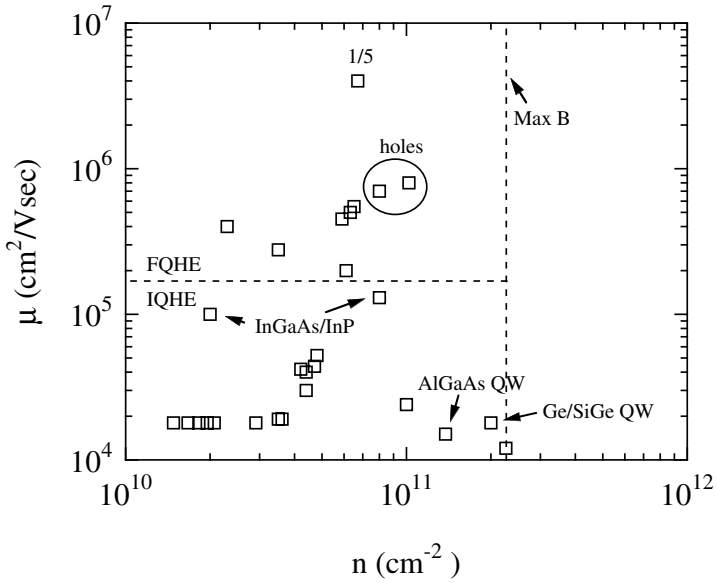

Figure 7. Mobility versus density for some of the samples in this study. The vertical dashed line indicated by Max B represents the maximum density for which the QH–insulator transition can be observed in our 15.5 T magnet. The horizontal dashed line approximately separates samples that do not exhibit the fractional QH phases from those that do. p-type samples are circled, and the samples labelled 1/5 exhibit the re-entrant insulating transition which we do not discuss in this paper.

from six different sources including three molecular beam epitaxy (MBE), one liquid-phase epitaxy (LPE) and two metallo-organic chemical vapour deposition (MO-CVD) machines. To ensure that geometrical factors, which are known to introduce modifications to transport in

the QH regime, do not come into play in our study, we did not maintain a uniform sample geometry. Rather, our samples were cut in many different shapes: some were wet etched into a Hall-bar shape of various dimensions, and others were cleaved into a square or rectangular shape with contacts diffused along the edges. The smallest contact-to-contact dimension was 100 μm while the largest was 1 mm. We also did not adhere to a specific structure design of the wafers, with diverse 2DESs embedded in GaAs/AlGaAs heterostructures and quantum wells (QWs), InGaAs/InAlAs QWs, InGaAs/InP heterostructures, AlAs/GaAs QWs, Ge/SiGe QWs, and Si MOSFETs. The total number of samples studied at low temperatures exceeds 150. Measurements performed included both the diagonal (ρ_{xx}) and off-diagonal, or Hall (ρ_{xy}) components of the resistivity tensor.

Quite generally, the QH series terminates, at high B, with a transition to an insulating phase. A typical transition is shown in figure 8, where we plot B-traces of ρ_{xx}, taken at several Ts. The samples exhibit metallic behaviour at low B followed by a set of integer QH states manifested by the vanishing of ρ_{xx}. As B is further increased beyond $\nu = 1$, ρ_{xx} increases for all temperatures. If we examine, however, the T-dependence of ρ_{xx} focusing on the high-B region (figure 9), we observe a stark change in its character: in the QH region, ρ_{xx} decreases as T is reduced towards absolute zero, while at higher B the opposite occurs, namely ρ_{xx} increases as $T \to 0$. It is therefore reasonable to use the temperature coefficient of resistivity (TCR) to delineate two different transport regimes: the QH state (TCR < 0) and the insulator (TCR > 0). We adopt this empirical 'definition' of the phases for the rest of the experimental section.

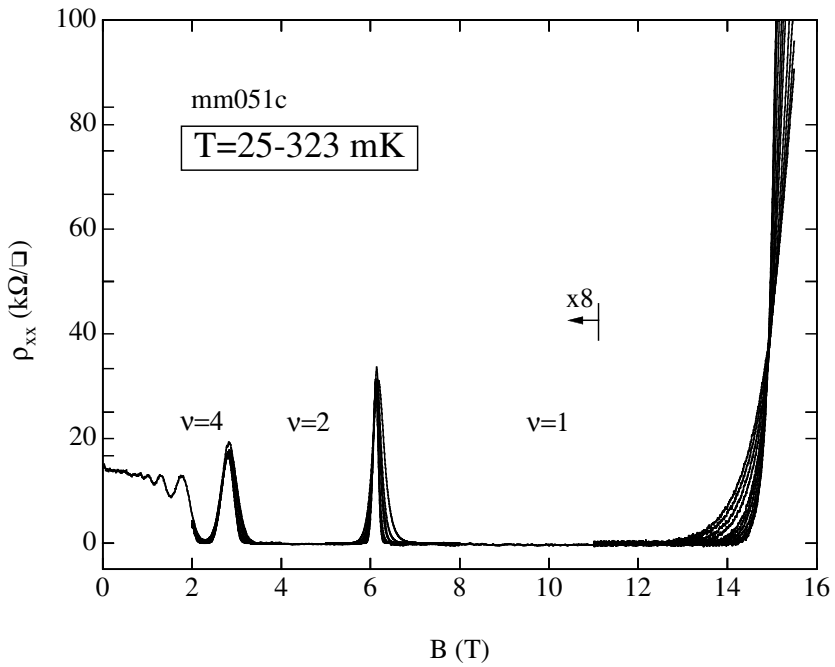

Figure 8. B-traces of ρ_{xx} at T = 25, 42, 62, 84, 106, 125, 145, 194, 238, 284, 323 mK, for a GaAs/AlGaAs sample mm051c. The mobility of this sample is 12 000 cm^2 V^{-1} s^{-1}.

Examining figure 9 further reveals another transport feature which is typical of the QH-to-insulator transition. It is possible, at low T, to identify a clear and well-defined B-value for which the TCR vanishes, within experimental error. The existence of this critical B-value (B_c)

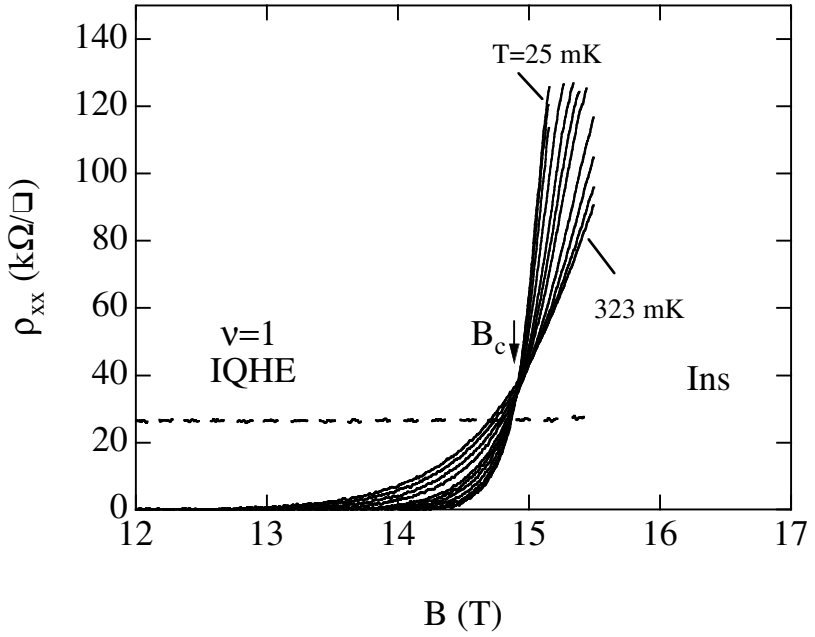

Figure 9. As figure 8, but for a narrow B-range focusing on the transition. We have also included a ρ_{xy}-trace (dashed curve).

allows us to unambiguously determine (subject to the definition of the previous paragraph) the boundary between the QH state and the insulator. A complete phase diagram can be obtained by following the position of this 'crossing' point as other relevant parameters, such as disorder or n, are changed, as was done extensively by Wong *et al* [9], Song *et al* [45] and others.

In a recent paper, Shahar *et al* [11] reported on a study of the ρ_{xx}-value at B_c (ρ_{xxc}) for a large collection of samples. They noticed that, in accordance with theoretical expectations [20], ρ_{xxc} seems to be close to the quantum unit of resistance, h/e^2, independent of sample parameters. Further, they showed that this apparent universality holds also for transitions from the $1/3$ fractional QH state to the insulator, again in agreement with theoretical predictions [19].

In the remainder of this section we expand on these previous findings by concentrating on the transport properties at the critical point. We will provide further evidence for the notion of universality near the QH-to-insulator transition, and remark on the QH–QH transitions. We will also closely examine the transport at the critical point and show that, at higher temperatures, systematic deviations of ρ_{xx} are clearly seen, although their trend and magnitude are sample dependent. Finally, we will discuss the disorder-driven QH–insulator transition which is realized experimentally by changing n by means of a metallic front-gate [4]. We will emphasize the similarities between the disorder-driven and magnetic-field-driven transitions.

We would like to precede the discussion of our data with a note of caution. It would be an unreasonable expectation to anticipate that *all* samples will behave uniformly in any subset of their transport characteristics. It is well known, for instance, that samples exhibiting the FQHE do not undergo a transition from the $\nu = 1$ IQHE to an insulator (they will, ultimately, undergo a transition to an insulator at higher B from a FQHE state). We therefore need to define clearly which subset of our samples will be included in our test for universality at the QH-to-insulator transitions. To clarify this need we plot, in figure 10, B-traces of ρ_{xx} taken at several temperatures for a GaAs/AlGaAs sample grown on a (311)A substrate to produce

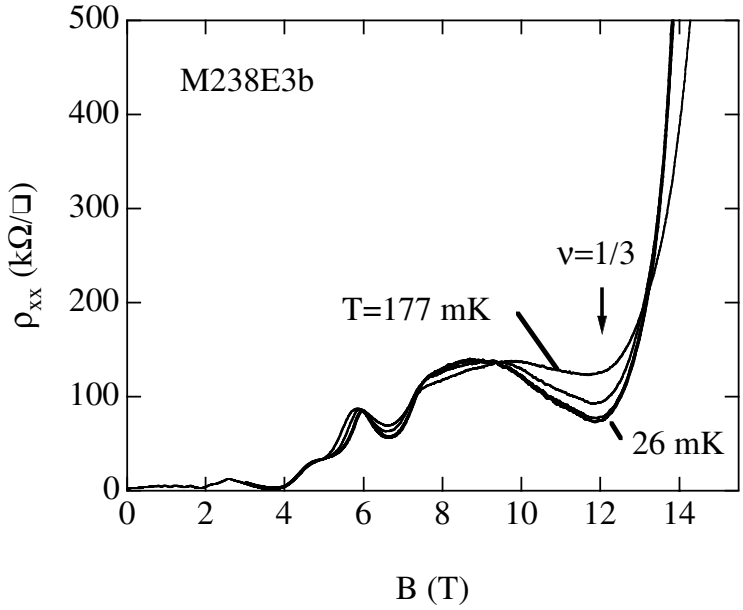

Figure 10. B-traces of ρ_{xx} at $T = 26$, 46, 55, 99, and 177 mK for a p-type GaAs/AlGaAs sample grown on a (311)A substrate. Note the apparent crossing point at 220 kΩ. $\mu = 220\,000$ cm^2 V^{-1} s^{-1}.

hole carriers. The 'QH' state marked on the figure as $1/3$ is clearly abnormal with a very high minimum resistivity at the lowest T. It is not surprising that the following 'transition' (common crossing point of the different T-traces) to an insulator is at a very high value, $\rho_{xxc} = 220$ kΩ, which significantly deviates from universality. The above discussion leads to a natural, albeit arbitrary, criterion for the 'suitability' of a given transition for a test of universality: for a transition to be considered, we require that it exhibit a fully developed QH state followed by a strong insulating behaviour. In both cases different tests can be considered to define the 'strength' of the phase. We have chosen for the QH phase a resistivity that decreases exponentially with decreasing T and, in addition, a value of ρ_{xx} at the QH minimum less than $h/100e^2$ at our lowest T, such that it is indistinguishable from zero when plotted on a scale which includes the transition point. Similarly we define it as a fully developed insulator if ρ_{xx} increases monotonically with B and reaches a value greater than $100h/e^2$ at our lowest T. Arbitrary as they are, these simple criteria safely eliminate from consideration samples like that of figure 10. Our results are not sensitive to small changes (factor of 2, for example) of our threshold values.

In a previous letter [11] we reported the observation of a universal value of ρ_{xxc}. In figure 11 we plot ρ_{xxc} versus B_c for 20 of our samples. In fact, other abscissas could have equally been used, such as μ or n, as ρ_{xxc} is rather independent of sample parameters and appears to be scattered around h/e^2 (solid line in figure 11). Two points should be emphasized. First, as we noted before [11], the ρ_{xxc}-value does not significantly differ between samples that undergo the transition from the $\nu = 1$ integer QH state (empty symbols) and those for which the transition takes place from the $\nu = 1/3$ fractional QH state (solid symbols). This is in agreement with the theoretical notion of super-universality [19]. We will not be discussing fractional QH transitions in the remainder of this paper.

Second, the data points are scattered over a relatively wide range of ≈15% around h/e^2.

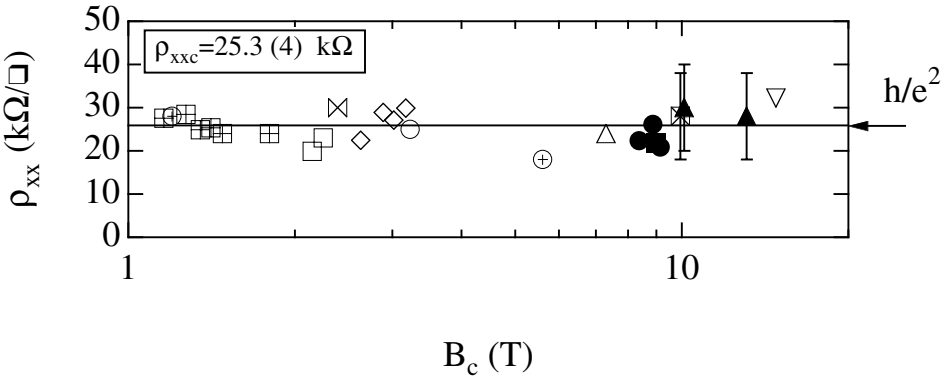

Figure 11. ρ_{xxc} versus B_c for some of our samples. Empty (filled) symbols are for transitions from the $\nu = 1$ IQHE ($\nu = 1/3$ FQHE) state. The error bars are typically smaller than the symbol size, except for the samples where they are indicated, which had ill-defined geometries.

This scatter is evident not only for different samples but also for different cool-downs of the same sample. Such variation would be expected in the mesoscopic regime, where sample dimensions are smaller than length scales set by the non-zero temperatures; different cool-downs would, in effect, be producing different samples. However, the cool-down dependence of ρ_{xxc} is puzzling if we recall that the samples are all of rather large size. This point has been emphasized in reference [11], and will be further discussed in section 4.

So far, we have reviewed our definition of the transition B_c and discussed the low-T value of ρ_{xxc}. We now proceed to discuss the T-dependence of ρ_{xxc} at higher temperatures. In figure 12 we plot ρ_{xxc} versus T for several samples. Depending on the sample and the T-range, different forms of behaviour are observed. Common to all samples is a certain range at the lowest T where ρ_{xxc} is T-independent, as expected at the critical point of the transition. This value of ρ_{xxc} is the value plotted in figure 11. As T is increased, systematic deviations

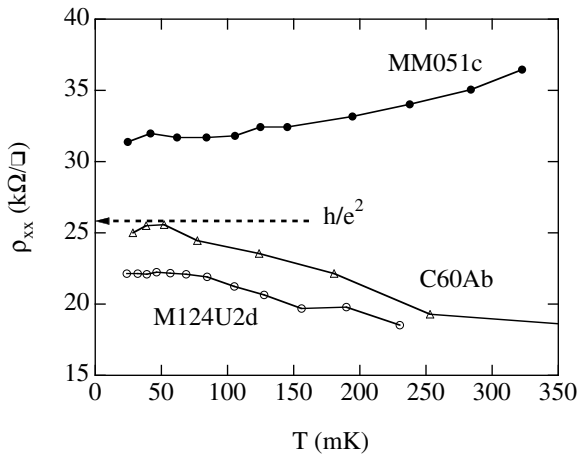

Figure 12. ρ_{xxc} at B_c, ρ_{xx}, versus T for three of our samples. The dashed arrow indicates the theoretically predicted value for the transition, h/e^2. Sample m124u2d is of higher mobility ($\mu = 500\,000$ cm^2 V^{-1} s^{-1}) and it exhibits the fractional QH effect. The data depicted are from the $\nu = 1/3$–insulator transition.

are observed for most samples. The T where these deviations appear is sample dependent, as is the trend which they take. In figure 13 we plot ρ_{xxc} versus T on a log scale which shows that for this particular sample, where we have a relatively wide range of data, a logarithmic T-dependence of ρ_{xxc} is a reasonable description of the data. This dependence is similar to that observed for 2D disordered metals at low T and $B = 0$. It is not clear whether the various mechanisms that lead to the logarithmic T-dependence at $B = 0$ are applicable for the high-B case. It is interesting to note that ρ_{xyc} has no noticeable T-dependence within this temperature range, and deviation from the low-T asymptotic value of ρ_{xyc} only appears at much higher temperatures [52].

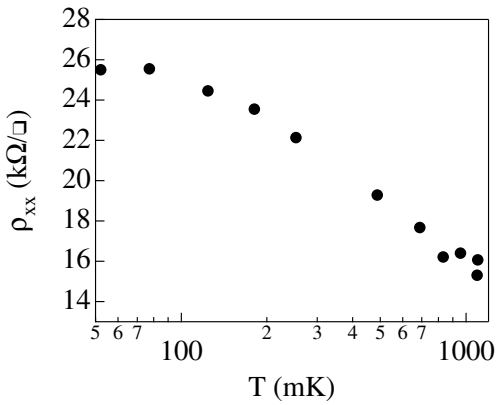

Figure 13. ρ_{xxc} versus T for sample C60Ab, with a log T scale. $\mu = 40000\ \mathrm{cm^2V^{-1}s^{-1}}$.

In the limit of strong disorder, the QH state ceases to exist and is replaced by an insulating behaviour. It is a reasonable expectation that, if one could vary the effective disorder over a wide enough range, a transition from a QH state to an insulator will be observed. This expectation was verified in experiments [4–6]. In fact, the disorder-induced transition was shown to be remarkably similar to the B-field-induced one as far as its critical properties are concerned [9]. To vary the effective disorder the experimentalist usually employs a metallic gate deposited near the 2D electrons. By biasing the gate with respect to the electron system n can be varied continuously, resulting in an effective disorder change via the dependence of the impurity potential strength on the screening effectiveness of the electrons which, in turn, depends on n. In figure 14 we plot ρ_{xxc} versus T in the vicinity of a disorder-induced $\nu = 1$-to-insulator transition. The different sets of data correspond, in this figure, to different gate-voltage bias and therefore to different disorder. The qualitative similarity to the B-induced transition is clear. In addition we note that ρ_{xxc} for this transition is 24 kΩ, again close to h/e^2. The T-range of our study in this case is not sufficient for detecting the high-T deviations of ρ_{xxc}.

Finally we remark on the behaviour at the critical point of QH–QH plateau-to-plateau transitions. As we demonstrated in a recent paper [15], a direct and clear relation exists between these transitions: it is possible to map the QH–QH transition to a QH-to-insulator transition by considering the former as a QH–insulator transition occurring at the top LL in the presence of an inert (full) bottom LL. In reference [15] we found that the transition point, when properly identified, is at a value which is close (within 20%) to the theoretically predicted value of $\frac{1}{5}\ h/e^2$ (see figure 15). Many other samples exhibit the QH–QH transition with ρ_{xxc} much smaller than expected [13]. We are uncertain why the QH–insulator transition yields a more consistent ρ_{xxc} than the QH–QH case; it may have to do with the fact that in the latter

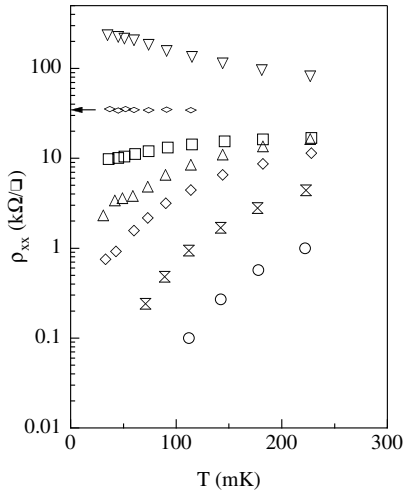

Figure 14. Disorder-induced QH–insulator transition. The densities are, from top to bottom, 0.7, 1.05, 1.3, 1.5, 1.7, 2.1, 2.9×10^{10} cm^{-2}.

case one needs to subtract out contributions from occupied Landau levels to the conductivity tensor, and then reverse the matrix to determine ρ_{xxc}.

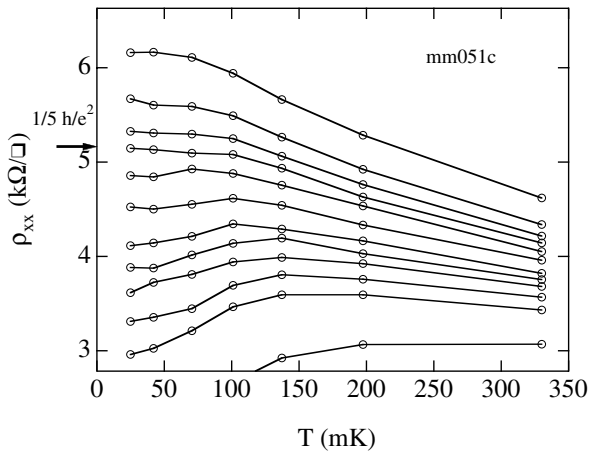

Figure 15. ρ_{xx} versus T near a QH–QH transition. For this transition the predicted critical ρ_{xx} is $1/5\ h/e^2$.

4. Discussion and comparison of experimental and numerical results

In this paper we have examined the issue of universality of the conductance tensor at quantum Hall transitions. The study is motivated on general grounds by the possibility of such universality of dimensionless quantities at quantum critical points. This possibility is further substantiated by our detailed study of a model of non-interacting electrons on a lattice, where we find that the Thouless conductance at critical points characterizing integer quantum Hall transitions is universal. This is in agreement with previous theoretical studies using different

models and approaches. It has been known for a long time that the Thouless conductance is closely related to the longitudinal conductivity of the system; they are believed to be of the same order of magnitude, no matter whether the system is in the insulating phase, metallic phase, or at the critical point, and are roughly proportional to each other. In the case of a *metallic* state at *zero* magnetic field, a rigorous proportionality between the two can be established [53]. More recent numerical work [54] has found proportionality between the Thouless conductance and Landauer–Büttiker conductance in Anderson models with long-stripe geometry, in both metallic and localized regimes, again at zero magnetic field. People have not succeeded, however, in establishing an exact relation between these two quantities in general. Thus while our finding of the Thouless conductance is clearly consistent with and strongly suggestive of a universal longitudinal conductivity of the system at the critical point, we cannot yet directly relate its value $g_T \approx 0.21$ to the experimental conductivity σ_{xxc} (or ρ_{xxc}). We do hope, however, that our finding here will motivate further theoretical work on the relation between these two quantities, in the quantum Hall regime. Indeed, if both of them are universal at the critical point, their ratio must also be universal at the critical point. Since numerically the Thouless conductance is much easier to calculate than the longitudinal conductivity, such a simple relation should be very useful in future research. It will also be very interesting to see if the same ratio relates these two quantities away from the critical point.

We have then tested this hypothesis by comparing with results of detailed experimental studies on the resistivity tensor at the points separating an integer quantum Hall phase and the high-magnetic-field insulator, as well as points separating different integer quantum Hall phases. We find that at the transition point between the $\nu = 1$ quantum Hall state and the high-magnetic-field insulating state, the longitudinal resistivity is clustered near h/e^2, the theoretically anticipated universal value [19]. This is in agreement with previous experimental studies, as well as general theoretical expectations. However, experimentally, we find a sizable scatter in the data for the longitudinal resistivity at the transition, about 15%. As pointed out earlier, this cannot be attributed to mesoscopic fluctuations, as all our samples are of fairly large size. Further, in the mesoscopic regime the resistivities are very sensitive to changes of B and other experimental knobs like gate voltage; such behaviour is not seen in our experiments. No such large scatter is seen in our numerical calculations, after sample-averaging is done. There are at least two important differences between our experimental and theoretical studies. First, electron–electron interactions are not taken into account in the theoretical model, whereas Coulomb interactions present in the experimental system are likely to be important to the critical behaviour [25, 26, 56]. Secondly, the way that the conductivity is averaged in our numerical work, albeit standard, may not necessarily be the most appropriate one for modelling the experiments. In the numerical study, we average the Thouless conductance over samples with the same size that are realizations of the random potential distribution under study. This would be a good way to model the real system, if the electric field in the sample (which, presumably, is broken into many incoherent pieces at finite T) is uniform. However, since the current tends to go through paths with minimum dissipation, it is likely that in real samples, the voltage drop (or electric field) as well as the current distribution are highly non-uniform, especially near the critical point. Possible effects of such non-uniform current and field distributions should be taken into account in any theory that attempts to explain the scattering of the data, as they are possibly related to the source of the scatter in the data. A model taking into account macroscopic inhomogeneities suggests that this may indeed be a source of 'non-universality' of the measured conductance at quantum Hall transitions [55].

Finally, we have, probably for the first time in the literature, presented a detailed analysis on how the $T = 0$ values of the resistivity tensor are approached in the asymptotic low-temperature regime, and the deviations at higher temperatures. We find that the longitudinal

resistivity ρ_{xx} at the critical point has some sizable, and apparently non-systematic, deviation from the asymptotic low-temperature value as the temperature is increased to a (relatively) high value; in the same temperature range, the Hall resistivity ρ_{xy} shows essentially no such deviation [52]. However, in our studies of the Thouless conductance, which is believed to be related to the diagonal conductance σ_{xx}, we saw very little change beyond a relatively small size. To clarify this seeming contradiction, let us consider the relation between the resistivity and conductivity tensors:

$$\rho_{xx} = \frac{\sigma_{xx}}{\sigma_{xx}^2 + \sigma_{xy}^2} \tag{4}$$

$$\rho_{xy} = \frac{\sigma_{xy}}{\sigma_{xx}^2 + \sigma_{xy}^2}. \tag{5}$$

If we imagine that at the critical point the values for a finite (but large) size L, $\sigma_{\mu\nu}(L)$ and $\rho_{\mu\nu}(L)$, differ from their universal values by (small) amounts $\delta\sigma_{\mu\nu}(L)$ and $\delta\rho_{\mu\nu}(L)$ respectively, then the above equations can be used to relate the deviations ρ_{xx} and ρ_{xy} from the universal values to the deviations of σ_{xx} and σ_{xy}. Retaining only the lowest-order† terms, we obtain

$$\delta\rho_{xx} \approx \frac{1}{\sigma_{xx}^2 + \sigma_{xy}^2}\left[\delta\sigma_{xx}\left(1 - \frac{2\sigma_{xx}^2}{\sigma_{xx}^2 + \sigma_{xy}^2}\right) - \delta\sigma_{xy}\frac{2\sigma_{xy}^2}{\sigma_{xx}^2 + \sigma_{xy}^2}\right] \tag{6}$$

$$\delta\rho_{xy} \approx \frac{1}{\sigma_{xx}^2 + \sigma_{xy}^2}\left[\delta\sigma_{xy}\left(1 - \frac{2\sigma_{xy}^2}{\sigma_{xx}^2 + \sigma_{xy}^2}\right) - \delta\sigma_{xx}\frac{2\sigma_{xx}^2}{\sigma_{xx}^2 + \sigma_{xy}^2}\right]. \tag{7}$$

At the integer quantum Hall–insulator transition, since $\sigma_{xyc} = \sigma_{xxc} = 0.5\, e^2/h$, this gives

$$\delta\rho_{xx} \approx -\delta\sigma_{xy}(2h^2/e^4) \tag{8}$$

$$\delta\rho_{xy} \approx -\delta\sigma_{xx}(2h^2/e^4) \tag{9}$$

i.e., the deviation of *longitudinal* resistivity $\delta\rho_{xx}$ at finite T is proportional to the deviation of *Hall* conductivity $\delta\sigma_{xy}$, while the absence of deviation in *Hall* resistivity implies the deviation of *longitudinal* conductivity $\delta\sigma_{xx} \approx 0$, consistent with our numerical study on Thouless conductance! Furthermore, in a non-interacting electron model, $\delta\sigma_{xy}$ at the critical point due to finite-size effects can only come from particle–hole asymmetry in the corresponding Landau level (band). In experimental systems, one expects, in general, asymmetry in the underlying potential, as well as mixing of different Landau levels (bands), both of which give rise to particle–hole asymmetry. Thus it is not unreasonable to expect finite-size corrections to σ_{xyc} (and consequently ρ_{xxc}) to be discernible.

Much as this simple correlation is appealing, this is not the whole story. This is because the calculated conductances as well as experimentally measured resistivities are ensemble-averaged quantities, $\langle\cdots\rangle$, over the random variable for a fixed size L. In the former case, the calculated quantity, $g_T(E_c)$, involves an ensemble-average $\langle\delta E\rangle$ over the change (due to boundary conditions) in the eigenenergies at the Fermi level, which is believed to be related to the ensemble averaged diagonal conductance $\langle\sigma_{xx}\rangle$ for the same size. In the case of experiment, non-zero temperature T sets a finite length scale L_T, and the sample may be thought of as an ensemble of samples of length L_T, and the measured longitudinal and Hall resistances are complicated averages of the corresponding quantities on the length scale L_T (which may lead to the non-uniform current and electric field distribution discussed above). Even for the case of a long sample with constant current, where one measures roughly $\langle\rho_{xx}\rangle$, no

† Since the observed deviation at finite T is typically of order one per cent of the asymptotic value, expansion to the lowest order should be sufficient.

equation analogous to equation (4) exists for the ensemble-averaged quantities; consequently the deviations for finite size cannot be related simply as was done above without averaging. Consequently, if the observed correlation exists between the finite-size corrections of $\langle\sigma_{xx}\rangle$ and $\langle\rho_{xy}\rangle$, it is for more complicated, and possibly much more interesting reasons. We also note in passing that it has recently been suggested [56] that scaling at QH transitions involves two dynamical exponents, of which one, related to the critical exponent η characterizing the eigenfunction correlation at the critical point, determines the departure from universal values of the conductance tensor, as a function of system size. We have mostly focused on a correlation involving the relative magnitudes of the departures for the averaged conductance and measured resistivity tensors; clearly, a more detailed investigation would be needed to address the critical exponent associated with the functional form of these departures from universality. Thus, while many features of the fascinating phase transitions in the quantum Hall regime, and their possible connection to quantum critical phenomena, have been explored and understood, there remain tantalizing and mysterious connections (as well as equally inexplicable disagreement) between various results which we expect will continue to provide challenging and fruitful areas of future research.

Acknowledgments

We acknowledge useful discussions with D Polyakov and S L Sondhi. This work was supported by NSF grant DMR-9400362. Part of this work was performed at the Aspen Center for Physics, during the Workshop on Quantum Phase Transition in Disordered Systems, in the summer of 1997.

References

[1] For a recent review that is particularly relevant to the present work, see Sondhi S L, Girvin S M, Carini J P and Shahar D 1997 *Rev. Mod. Phys.* **69** 315
[2] Wei H P, Tsui D C, Paalanen M A and Pruisken A M M 1988 *Phys. Rev. Lett.* **61** 1294
[3] Koch S *et al* 1991 *Phys. Rev. Lett.* **67** 883
[4] Jiang H W *et al* 1993 *Phys. Rev. Lett.* **71** 1439
[5] Wang T *et al* 1994 *Phys. Rev. Lett.* **72** 709
[6] Hughes R J F *et al* 1994 *J. Phys.: Condens. Matter* **6** 4763
[7] Alphenaar B W and Williams D A 1994 *Phys. Rev.* B **50** 5795
[8] Wei H P *et al* 1994 *Phys. Rev.* B **50** 14 609
[9] Wong L W, Jiang H W, Trivedi N and Palm E 1995 *Phys. Rev.* B **51** 18 033
[10] Pan W, Shahar D, Tsui D C, Wei H P and Razeghi M 1997 *Phys. Rev.* B **55** 15 431
[11] Shahar D, Tsui D C, Shayegan M, Bhatt R N and Cunningham J E 1995 *Phys. Rev. Lett.* **74** 4511
[12] Okamoto T, Shinohara Y and Kawaji S 1995 *Phys. Rev.* B **52** 11 109
[13] Rokhinson L P, Su B and Goldman V J 1995 *Solid State Commun.* **96** 309
[14] Shahar D, Tsui D C, Shayegan M, Cunningham J E, Shimshoni E and Sondhi S L 1996 *Science* **274** 589
[15] Shahar D, Tsui D C, Shayegan M, Shimshoni E and Sondhi S L 1997 *Phys. Rev. Lett.* **79** 479
[16] Chalker J T and Coddington P D 1988 *J. Phys. C: Solid State Phys.* **21** 2665
[17] Huckestein B and Kramer B 1990 *Phys. Rev. Lett.* **64** 1437
[18] Huo Y and Bhatt R N 1992 *Phys. Rev. Lett.* **68** 1375
[19] Kivelson S, Lee D H and Zhang S-C 1992 *Phys. Rev.* B **46** 2223
[20] Huo Y, Hetzel R E and Bhatt R N 1993 *Phys. Rev. Lett.* **70** 481
[21] Lee D-H, Wang Z and Kivelson S 1993 *Phys. Rev. Lett.* **70** 4130
[22] Wang Z, Lee D-H and Wen X-G 1994 *Phys. Rev. Lett.* **72** 2454
[23] Liu D and Das Sarma S 1994 *Phys. Rev.* B **49** 2677
[24] Ludwig A W W, Fisher M P A, Shankar R and Grinstein G 1994 *Phys. Rev.* B **50** 7526
[25] Yang S-R E, MacDonald A H and Huckestein B 1995 *Phys. Rev. Lett.* **74** 3229
[26] Lee D-H and Wang Z 1996 *Phys. Rev. Lett.* **76** 4014

[27] Lee D-H and Wang Z 1996 *Phil. Mag. Lett.* **73** 145
[28] Wang Z, Jovanovic B and Lee D-H 1996 *Phys. Rev. Lett.* **77** 4426
[29] Cho S and Fisher M P A 1997 *Phys. Rev.* B **55** 1637
[30] Ando T 1989 *Phys. Rev.* B **40** 5325
[31] Tan Y 1994 *J. Phys.: Condens. Matter* **6** 7941
[32] Liu D Z, Xie X C and Niu Q 1996 *Phys. Rev. Lett.* **76** 975
[33] Yang K and Bhatt R N 1996 *Phys. Rev. Lett.* **76** 1316
Yang K and Bhatt R N 1999 *Phys. Rev.* B **59** 8144
[34] Xie X C *et al* 1996 *Phys. Rev.* B **54** 4966
[35] Haldane F D M and Yang K 1997 *Phys. Rev. Lett.* **78** 298
[36] Sheng D N and Weng Z Y 1997 *Phys. Rev. Lett.* **78** 318
[37] Sorensen E S and MacDonald A H 1996 *Phys. Rev.* B **54** 10 675
[38] Guo Muyu and Bhatt R N, unpublished
[39] Sachdev S 1998 *Phys. Rev.* B **57** 7157
[40] Sheng D N and Weng Z Y 1998 *Phys. Rev. Lett.* **80** 580
[41] Fisher M P A, Grinstein G and Girvin S M 1990 *Phys. Rev. Lett.* **64** 587
[42] Shahar D *et al* 1998 *Solid State Commun.* **107** 19
[43] Edwards J T and Thouless D J 1972 *J. Phys. C: Solid State Phys.* **5** 807
Thouless D J 1974 *Phys. Rep.* **13** 93
[44] Huckestein B 1994 *Phys. Rev. Lett.* **72** 1080
[45] Song S-H, Shahar D, Tsui D C, Xie Y H and Monroe D 1997 *Phys. Rev. Lett.* **78** 2200
[46] Lee P A and Ramakrishnan T V 1985 *Rev. Mod. Phys.* **57** 287
[47] Liu Y *et al* 1993 *Phys. Rev.* B **47** and references therein
Hebard A F and Paalanen M A 1990 *Phys. Rev. Lett.* **65** 927
[48] Jain J K 1989 *Phys. Rev. Lett.* **63** 199
[49] Simonian D, Kravchenko S V and Sarachik M P 1997 *Phys. Rev.* B **55** R13 421
[50] Abrahams E *et al* 1979 *Phys. Rev. Lett.* **42** 673
[51] Shahar D 1996 *PhD Thesis* Princeton University, NJ
[52] See, e.g., Hilke M, Shahar D, Song S H, Tsui D C, Xie Y H and Monroe D 1998 *Nature* **395** 675
[53] Akkermans E and Montambaux G 1992 *Phys. Rev. Lett.* **68** 642
[54] Braun D, Hofstetter E, Montambaux G and MacKinnon A 1997 *Phys. Rev.* B **55** 7557
[55] Ruzin I M, Cooper N R and Halperin B I 1996 *Phys. Rev.* B **53** 1558
[56] Polyakov D G and Samokhin K V 1998 *Phys. Rev. Lett.* **80** 1509
Polyakov D G 1998 *Phys. Rev. Lett.* **81** 4696